Mitotic Golgi Fragments in HeLa Cells and Their Role in the Reassembly Pathway

John M Lucocq, Eric G. Berger* and Graham Warren

Department of Biochemistry, University of Dundee, Dundee DD1 4HN, Scotland; and *Physiologisches Institut, Universität Zürich, CH-8057 Zürich, Switzerland

Abstract. Immunoelectron microscopy and stereology were used to identify and quantitate Golgi fragments in metaphase HeLa cells and to study Golgi reassembly during telophase. On ultrathin frozen sections of metaphase cells, labeling for the Golgi marker protein, galactosyltransferase, was found over multivesicular Golgi clusters and free vesicles that were found mainly in the mitotic spindle region. The density of Golgi cluster membrane varied from cell to cell and was inversely related to the density of free vesicles in the spindle. There were thousands of free Golgi vesicles and they comprised a significant proportion of the total Golgi membrane.

During telophase, the distribution of galactosyltransferase labeling shifted from free Golgi vesicles towards Golgi clusters and the population of free vesicles was depleted. The number of clusters was no more than in metaphase cells so the observed fourfold increase in membrane surface meant that individual clusters had increased in size. More than half of these had cisterna(e) and were located next to "buds" on the endoplasmic reticulum. Early in G1 the number of clusters dropped as they congregated in the juxtanuclear region and fused.

These results show that fragmentation of the Golgi apparatus yields Golgi clusters and free vesicles and reassembly from these fragments is at least a two-step process: (*a*) growth of a limited number of dispersed clusters by accretion and fusion of vesicles to form cisternal clusters next to membranous "buds" on the endoplasmic reticulum; (*b*) congregation and fusion to form the interphase Golgi stack in the juxtanuclear region.

ANIMAL cells have a juxtanuclear Golgi apparatus comprising stacks of cisternae that are extensively interconnected (Novikoff et al., 1971; Rambourg et al., 1974, 1979, 1981). Early in mitosis, the Golgi apparatus fragments extensively, the fragments are dispersed throughout the mitotic cell cytoplasm and a smaller Golgi apparatus is rebuilt during telophase in each daughter cell (Burke et al., 1982; Hiller and Weber, 1982). To fully understand the process of Golgi division, all types of fragments must be identified.

We have been able to identify one type of fragment that is found in mitotic HeLa cells (Lucocq et al., 1987). These are globular clusters of vesicles and tubules that we termed Golgi clusters. They contain the *trans*-Golgi marker galactosyltransferase (Roth and Berger, 1982) and are true products of the fragmentation process because they are more numerous than the interphase Golgi apparatus (Lucocq and Warren, 1987). However, the exact role and importance of the clusters in Golgi division is unclear because they may not be the only type of Golgi fragment and may not even be the major one. Another candidate for a Golgi fragment is the free vesicle, large numbers of which have been observed during mitosis (Zeligs and Wollman, 1979) though their origin was not determined. Unfortunately, in our previous study (Lucocq et al., 1987), we were unable to visualize such small vesicles (50–100 nm in diameter) because of limitations in the embedding technique. We were therefore unable to determine whether they contained galactosyltransferase. In this study we have used ultrathin frozen sections to visualize all of the possible Golgi fragments including small, dispersed vesicles. By combining this technique with stereology on epoxy resin sections we have also been able to work out the way in which these fragments reform the interphase Golgi apparatus.

Graham Warren's present address is Imperial Cancer Research Fund, P. O. Box 123, Lincoln's Inn Fields, London WC2A 3PX.

Materials and Methods

Cells

Mitotic Hela cells were isolated as previously described (Lucocq et al., 1987). Cells were sedimented by centrifugation at ~1,000 *g* for 4 min at 37°C and fixed as described below.

Preparation for Electron Microscopy

Unless otherwise stated all preparation steps were performed at room tem-

perature. Observations were made and micrographs taken on a JEOL 1200 EX electron microscope at 60kV.

Cell pellets destined for stereology were fixed in 0.5% glutaraldehyde in cacodylate buffer (0.1 M cacodylate/HCl buffer, pH 7.4) containing 5% (wt/vol) sucrose, for 30 min. After rinses in cacodylate buffer, the pellets were postfixed in 1% OsO_4/1.5% potassium ferrocyanide in cacodylate buffer for 30 min, washed briefly in cacodylate buffer, dehydrated in graded ethanols, and embedded in Epon 812 equivalent obtained from TAAB Laboratories (Berks, England). Sections ~40 nm thick were mounted on formvar/carbon-coated slot grids (1 × 2 mm) according to Galey and Nilsson (1966) and stained with lead citrate for 5 min.

Ultrathin frozen sections were prepared from cell pellets (from three separate cultures) fixed in 0.5% glutaraldehyde in 0.2 M Pipes, pH 7.2, for 30 min. Pellets were infiltrated with 2.1 M sucrose in PBS (10 mM NaPi, 150 mM NaCl, pH 7.4) for 15–30 min on ice and frozen in liquid nitrogen. Sections were cut at −110°C with glass knives in an Fc4 cryoattachment on a Reichert Ultracut E microtome. They were mounted on formvar/carbon-coated nickel 150 mesh grids and stored on 0.5% fish skin gelatin (Sigma Chemical Co., Poole, England) in PBS (PBS/gelatin) at 4°C for a maximum of 18 h.

Immunoelectron Microscopy

All steps were performed at room temperature. Ultrathin sections were floated on 0.1 M NH_4Cl in PBS for 5 min, then on PBS/gelatin for 5 min, and then on affinity purified anti-galactosyltransferase antibodies (Roth and Berger, 1982), diluted in PBS/gelatin, for 30 min. After six washes on PBS (15 min total) sections were incubated on protein A-gold (5 nm gold) diluted in PBS/gelatin for 30 min and washed on PBS (six changes, 30 min total).

Sections were contrasted and embedded in Epon 812 equivalent according to Keller et al. (1984) as follows. After three washes in 0.2 M cacodylate/HCl buffer, pH 7.4, the sections were fixed again for 30 min in 0.5% glutaraldehyde in cacodylate buffer containing 5% (wt/vol) sucrose. Grids were then floated on 1% OsO_4/1.5% potassium ferrocyanide in cacodylate buffer for 30 min. After a brief wash in cacodylate buffer, sections were dehydrated in graded ethanols of 70, 90, and 100% ([vol/vol] 2 min each) and infiltrated with two changes of 20% (vol/vol) Epon/ethanol (40 min total). Grids were then blotted firmly between two pieces of filter paper (No. 50; Whatman Inc., Clifton, NJ) and then left at room temperature for 30 min before polymerizing the resin at 60°C for 15–18 h. Sections were stained with Reynolds lead citrate for 5–10 min.

Controls were performed by omitting the antibody and also by replacing it with an antiserum against rat liver sialyltransferase (gift from Dr. J. Paulson, University of California) that labeled rat liver Golgi but not HeLa cell Golgi cisternae. Golgi clusters were not labeled under these conditions.

Golgi clusters from metaphase and telophase cells were sampled using unbiased counting frames (Gundersen, 1977) placed systematic random across the pellet profile and photographed at a calibrated magnification of 25,000. The whole profile of selected clusters was photographed to allow the proportion of cluster profiles that were labeled to be determined. Areas for background counts were photographed in systematic random positions over the cell pellet at the same magnification as used for clusters. Metaphase cells were any cell with equatorial chromosomes and telophase any cell with a reforming or complete nuclear envelope and an elongated nucleus.

Cluster area was estimated by point counting using grid B (see Stereology section below) and the cluster area was defined as that area enclosed by any group of at least five vesicular profiles, and/or at least one cisterna, with each component less than two vesicle widths from any other cluster component. In this paper we define any vesicular profile as one having an axial ratio of less than one to four and so these profiles contain the less frequent tubular profiles we have described in a previous publication (Lucocq et al., 1987). Any structure with an axial ratio greater than one to four was considered cisternal. Peripherally situated clusters of vesicles close to the plasma membrane were not included in the quantitative analysis because they were not labeled. These contained larger electron lucent vesicular profiles sometimes interconnected and often continuous with the plasma membrane.

The proportion of clusters that were labeled was found in the following way. The expected total number of gold particles due to background was calculated from the product of the total area of the clusters and the known mean background labeling density over the cytoplasm. This number of gold particles was then taken from the labeling over clusters by arranging the cluster data linearly and removing every nth gold particle, where n = total labeling divided by calculated number of background particles. About one in every 30 particles were removed. Those clusters with remaining gold particles were considered labeled. It is important to point out that because big clusters are more likely to appear in sections than small ones these proportions tend to be derived from the larger clusters in the cluster population.

Vesicles were defined as any group containing less than five vesicle profiles. The density of labeling over vesicles was found from the number of gold particles associated with vesicular profiles in spindle regions selected with unbiased counting frames and the expected area occupied by vesicles of these spindles. The latter was estimated by point counting on 40-nm-thick sections of cell pellets processed for stereology. These sections were used because vesicles were difficult to visualize in frozen sections and an underestimate of vesicle area would give an artificially high value for the labeling density.

The number of gold particles over vesicles in the spindle, and therefore the number of labeled vesicles (the vast majority of vesicles had only one particle associated with them) was calculated from: the labeling density in gold particles over vesicles/μm^2 of spindle; the spindle volume estimated by point counting on systematic sections of cells selected by disectors (see below); and a section thickness of 100 nm for the frozen sections.

The number of gold particles over clusters in metaphase and telophase cells was calculated from the labeling density over the clusters, the volume of cluster in the cell, and a section thickness of 100 nm.

Sampling of Cells for Stereology

The mitotic cells were at all stages of mitosis. To select mitotic stages from the population we used the disector (Sterio, 1984). This three-dimensional probe selects cells with equal chance, irrespective of their sizes, and overcomes the problem that larger cells have more chance of being in a section. Particles (in this case cells) are sampled or counted if (*a*) they intersect one of two parallel planes (or sections) and are selected by its unbiased two-dimensional counting frame, and (*b*) do not intersect the second parallel plane, termed the "look up" plane.

A stack of 13 sections, each exactly 40 or 50 sections from the next (~2 μm), was prepared. The stack had a height (~26 μm) that was larger than the largest mitotic cell profile (~22 μm). It was prepared at a random position in the block. On the second section the whole pellet profile was included where possible but when artificial edges were present, two-dimensional unbiased counting rules were applied with appropriate counting frames (Sterio, 1984). Cells were sampled if their profiles were in the second section or its counting frame but not present in the first "look up" section.

Selected cells of the stack were assigned to one of three stages: (*a*) Metaphase cells had condensed chromosomes without a nuclear envelope. In practice 88% had equatorial chromosomes and were clearly metaphase whereas the remainder were either prometaphase cells or metaphase cells sectioned in the plane of the equatorial plate. (*b*) Telophase cells had profiles with a forming or complete nuclear envelope and an elongated nucleus. These elongated profiles are derived from disk shaped nuclei that when sectioned in the plane of the disk appear round, not elongated. To avoid excluding data from these cells we attempted to identify them by including cell profiles with the center of their nuclear profiles in a maximum of two sections of the stack. This effectively includes telophase cells that are sectioned in the plane of their disk-shaped nuclei and excludes G1 cells which have nuclei present in three or more sections of the stack. (*c*) Early G1 cells had round nuclear profiles present in more than two sections of the stack and usually possessed evidence of nucleolar condensation. When the number of cells exceeded the required number they were subsampled systematic random in a constant direction across the pellet.

Stereology

From each of three separate cultures, small fragments of pellet were embedded in epoxy resin. For this study we have assumed that the mainly spherical mitotic cells are each randomly oriented in the pellet. Calibrations were carried out using a line grating replica with 2,160 lines/mm. Coefficients of variation (CV)[1] for ratio estimates were computed according to Cochran (1977).

Three square lattice grids were used for stereological estimations. These had the following point to point spacings: grid A, 4.96 mm; grid B, 2.5 mm; and grid C, 1.0 mm. Section thickness was estimated by the method of Small (1968). Cell volume was estimated by the Cavalieri principle orchestrated for point counting in three dimensions (Gundersen, 1986). Estimates were made from micrographs of whole cell profiles observed at a final calibrated magnification of 40,000. These were obtained from the stack of sections cut

1. *Abbreviation used in this paper*: CV, coefficient of variation.

to select and stage the cells (see above). Knowing the distance (H) between sections of the stack and the area (a) associated with points (P) of a square grid lattice (grid A), the volume of each systematically sectioned cell can be found from $V_{cell} = a \times H \times \Sigma P$. Summation of points is over all sections through the cell and $H = t \times K$, where t is the mean section thickness and K is the number of sections in the stack interval. The volume of the spindle was estimated in the same way. It was defined on sections as the area enclosed by cisternae of endoplasmic reticulum surrounding the spindle and excluding the chromosomes.

Volume density or volume fraction (V_v) of Golgi cluster (cl) in each individual cell, $V_{vcl,cell} = V_{cl}/V_{cell}$, was estimated by point counting (grid A and C) on micrographs of whole cell profiles examined at a final calibrated magnification of 40,000. An estimate of the $V_{vcl,cell}$ for the mitotic stage of the culture is $\Sigma V_{vcl,cell}$ divided by the number of cells. In a typical experiment we counted means of 22 points on clusters and 401 on the cell distributed over 6.5 sections per cell in metaphase cells, and 45 points on clusters, 180 on each cell spread over 5.2 sections per cell in telophase.

Surface density (S_v) of membrane in clusters of individual cells, $S_{vcl,cl} = S_{cl}/V_{cl}$, was determined from systematic random micrographs at a final calibrated magnification of 200,000. $2I/L$ gives $S_{vcl,cell}$ where I is the sum of intercepts of grid lines with the cluster membranes and L the line length applied. L is estimated from point counts over the cluster X distance between the points of a square lattice grid (grid B). Estimates varied little from cell to cell so, for example, a typical result from single cultures for $S_{vcl,cl}$ was 37 μm^{-1} (four cells, CV 6%) for metaphase cells and 36 μm^{-1} (three cells, CV 5%) for telophase cells.

$S_{vcl,cl}$ used in this paper is an overestimate of the surface density because the mean section thickness, 40.3 nm (three cultures, CV 14.6%), is similar to the diameter of the cluster vesicles (Weibel and Paumgartner, 1978), which was 51.9 nm (three cultures, CV 2.5%) for telophase and 49.2 nm (three cultures, CV 9.4%) for metaphase cells. The surface of membrane in telophase clusters is overestimated less because their cisternae are much bigger than the cluster vesicles. Thus the ratio of the telophase cluster membrane surface to that of metaphase cells is actually artificially low (see Results). Correction factors were applied only to give an impression of the real membrane surface (Weibel and Paumgartner, 1978). Knowing $S_{vcl,cl}$ for individual cells an estimate of the $S_{vcl,cl}$ for the culture can be found from Σ $S_{vcl,cell}$ divided by the number of cells, and membrane per cell for the culture equals $S_{vcl,cl} \times V_{vcl,cell} \times V_{cell}$.

Counting Golgi Clusters and Vesicles

Individual cells were selected by a disector and staged on a stack of sections as described above. The number of clusters was counted using small sets of serial sections placed systematically at ~2 (telophase) or 4 (metaphase) μm intervals in a random position between the stack sections used to select the cells. Whole profiles of selected cells were photographed at a calibrated magnification of 4,000. There were between four and six sections in each set. In turn each end section of the set was designated the "look-up" section and all clusters present in the other sections but not in the "look-up" section were counted (Q^-). Using the disector in both directions increases efficiency because different particles are counted in each direction. The number (N) of clusters in the individual cell was estimated independently from knowing the section thickness by $N_{cl,cell} = V_{cell}\Sigma Q^-/v_{dis}$. v_{dis} is the total volume of the disectors used to count the clusters. $V_{cell} = a \times H \times \Sigma P$ and $v_{dis} = a \times h \times \Sigma P$. Here, $H = K \times t$ and $h = 2k \times t$, where t is the mean section thickness, K is the number of sections in each stack interval, and k is (the number of sections in set) 1. So $N_{cl,cell} = \Sigma K \times \Sigma Q^-/\Sigma\ 2k$. Disectors composed of serial sections were made in this case to avoid missing small clusters situated between the end section and the "look-up" section of the set. On average 6.2% of the clusters in each metaphase cell were sampled.

The same cluster could be counted more than once if it is irregular in shape (nonconvex) because it might present more than one "top" in its periphery (each "top" counted as Q^-). In effect this would break an absolute requirement of the disector which is that a particle presenting itself as more than one profile must be identified as such. Since we could not identify irregular clusters in our small sets of sections this could have led to overestimation (bias) of the cluster number. We therefore used a series of 30 serial sections (see below) to count the ratio of $n_{cl,ser}/Q^-$ where $n_{cl,ser}$ is the actual number of clusters found in the serial sections. This ratio was 0.96 for telophase and 0.97 for metaphase. Estimates of cluster number were corrected accordingly to give $N_{cl,cell(corr)}$. Cluster volume for individual cells was estimated by $V_{cl} = V_{cell} \times V_{vcl,cell}/N_{cl,cell(corr)}$. Vesicle counting was not carried out using disectors. This is because densely packed, very small structures are difficult to locate in the look-up section especially when other reference structures are absent as is the case in the spindle. Instead, two different methods were used. (*a*) A counting method. All the sectioned vesicles that gave a clear membrane were counted. The estimated number per spindle (or cell) is the product of the total number counted in the stack of systematic sections and the number of sections in the stack interval. Using this method the same vesicle was only rarely found in two adjacent sections and counted twice (7.7% of total counts, 104 vesicles counted). We consider that this method is therefore unlikely to overestimate vesicle number. (*b*) These counts were checked by an indirect method. First, the volume of vesicles in the spindle was found by point counting to which correction factors for the effect of section thickness were applied (see below). The volume of individual vesicles was calculated from their diameter (57 nm, n = 16, CV 10.5%) assuming they were spheres and used with the estimate of total vesicle volume per spindle to compute the vesicle number. The counting method gave a mean value of 7,999 vesicles per cell (16 cells, CV 41%) compared to 10,092 (10 cells, CV 46%) for the indirect method, an increase of 1.26-fold. Only the results from the counting method are presented in this paper.

Serial Sections of Clusters

From blocks of two experiments, ≥30 serial sections were prepared and three metaphase and three telophase cells sampled by selecting their profiles with unbiased counting frames. Metaphase cells had a band of chromosomes across the middle whereas the telophase cells had an elongated nucleus.

This procedure selects larger cells with chromosomes or nuclei oriented perpendicularly to the plane of section. However, the resulting bias should be small because, (*a*) from the unbiased estimations described above we found that cell size is not significantly related (statistically) to estimates of cluster size and amount (unpublished data), (*b*) disector sampling and volume estimation are not orientation dependent, and (*c*) excluded sections contained only 13 and 15% of the cell volume in metaphase and telophase respectively.

These sections were used to estimate the $n_{cl,ser}/Q^-$ ratio (see above), quantify the proportion of clusters possessing cisternae and the proportion adjacent to membranous "buds" on the endoplasmic reticulum, and estimate the size distribution of the clusters. The first 15 sections were used as a disector to select the Golgi clusters with the first section of the series the "look-up" section. The remaining 15 or more sections were used to complete the volume estimations and identify cisternae and endoplasmic reticulum with membranous buds in selected clusters. Cluster size was estimated by the Cavalieri principle from point counting on prints (grid C) of negatives enlarged 2.7–3.0-fold taken at a calibrated magnification of 4,000.

The fraction of spindle vesicle labeling due to peripheral sections was estimated in the following way. The volume of cluster peripheries (less than five vesicles) in the spindle was found from their volume fraction in the spindle, obtained by point counting on the series of 30 sections, and the spindle volume found by point counting on the stacks of sections through the cells. The expected area of spindle clusters sectioned in the periphery by frozen sections (thickness ~100 nm) could then be found and the expected number of gold particles calculated and compared to the observed number of particles over vesicles.

Results

Structures Labeled for Galactosyltransferase in Frozen Sections

Clusters. In this study we used frozen sections to identify Golgi fragments in mitosis because they allow better visualization of membranes. Sections were labeled with a rabbit anti-galactosyltransferase antibody, affinity purified as previously described (Roth and Berger, 1982), followed by protein-A gold. The specificity of this antibody is shown in Fig. 1 where only *trans*-Golgi cisternae were labeled in interphase HeLa cells.

In metaphase HeLa cells specific labeling was found over clusters of vesicles (Fig. 2) much smaller than had been seen in thin sections of mitotic cells embedded in Lowicryl K4M (Lucocq et al., 1987). In our hands, small vesicles (~50 nm in diameter) are best visualized when immunolabeled frozen

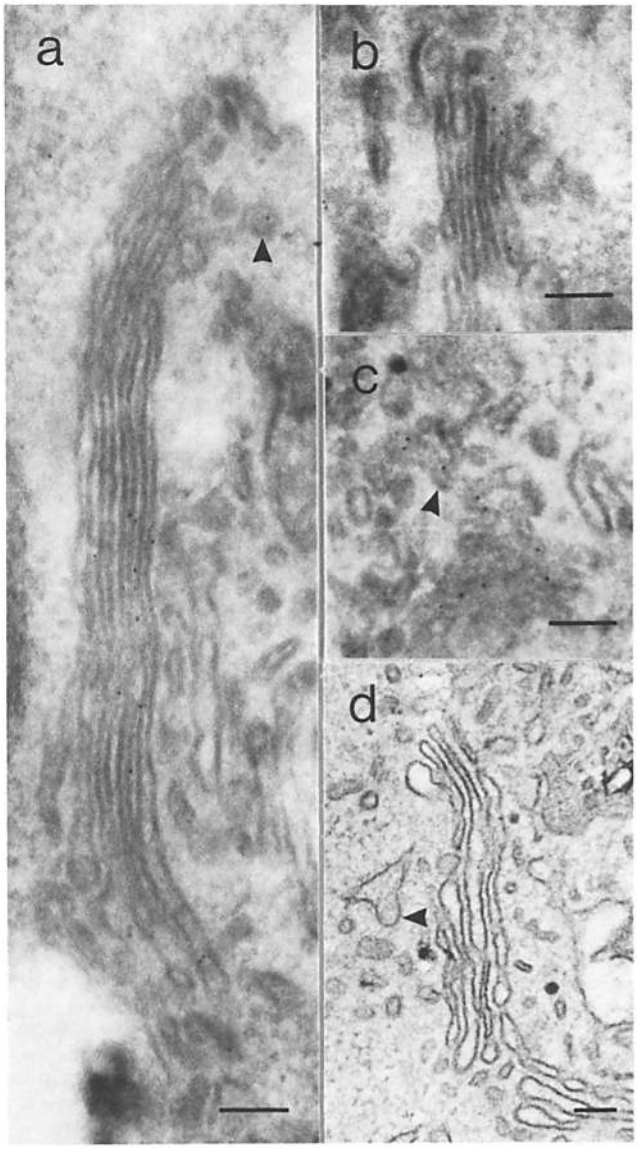

Figure 1. Interphase Golgi apparatus of HeLa cells. (*a–c*) Frozen sections; (*d*) epoxy resin section. Labeling for galactosyltransferase was located over one or two *trans* cisternae of the Golgi apparatus (*a* and *b*). Some noncisternal structures on the lateral aspect of *trans*-cisternae are also labeled (*arrowhead in a*) and these are seen as tubules when *trans*-cisternae are sectioned en face (*arrowhead in c*). (*d*) Membranes of the interphase Golgi stack are well-visualized in sections of cells processed for stereology. The arrowhead points to a bud on the endoplasmic reticulum. Bars, 200 nm.

sections are treated with osmium tetroxide and embedded in epoxy resin (Keller et al., 1984). Often, even the smallest clusters, with only a few vesicles, appeared to be labeled. These clusters only rarely had the large lucent vesicles which were a feature of the clusters seen in Lowicryl K4M–embedded cells. This is partly because smaller clusters lacking larger vesicles can be easily identified in frozen sections and also because large vesicles appear mainly in clusters in prometaphase cells, a stage that is rare in these preparations (see Materials and Methods). Examples of labeled clusters are shown in Fig. 2.

Clusters in telophase cells were not only clusters of vesicles but many of the labeled profiles also contained cisternae (Fig. 3).

Morphological Definition of Clusters. Quantitation of Golgi clusters is much easier to perform on cell pellets embedded in plastic because Golgi membranes are better visualized and serial sectioning can be performed. Examples of the structural preservation of Golgi membrane are given in Figs. 1 *d* and 2 *c*. We therefore chose morphological criteria that identified those Golgi clusters over which labeling for galactosyltransferase was concentrated in frozen sections. We then applied these criteria to quantitate Golgi clusters on sections of epoxy-embedded cells.

Labeled clusters with five or more vesicular profiles could be clearly identified in frozen sections. When there were fewer than five vesicular profiles, clusters were difficult to identify because the membranes of the vesicles were indistinct. A sectioned cluster was therefore identified as five or more vesicular profiles whether or not they had distinct membranes. Some labeled clusters in telophase cells had cisterna(e) in addition to vesicles and in some of these cases there were too few vesicles to meet the criterion. They were included by modifying the criterion to five or more vesicles and/or at least one cisterna.

Clusters identified using these morphological criteria alone had galactosyltransferase labeling concentrated over them. Collectively the Golgi clusters of metaphase and telophase cells showed much higher labeling than background over the rest of the cell giving a signal to background ratio between 30 and 50 (Table I). Individually, in three cultures, 61% (CV 15%) of the cluster profiles in metaphase and 83% (CV 19%) of the cluster profiles in telophase cells were labeled. These data show that the morphological criteria permitted identification of one type of Golgi fragment and allowed its quantitation using stereology.

Vesicles. To our surprise we found that vesicle profiles were also labeled for galactosyltransferase (Fig. 4). Even though 75% (three cultures, CV 13%) of the labeling for galactosyltransferase in metaphase cells was found over clusters containing five or more vesicles, the rest (25%, CV 36%) was situated over smaller groups of vesicles and single vesicle profiles, the latter being the most numerous (Fig. 4). Most of these vesicle profiles were in the spindle region of metaphase cells (Fig. 2, *d* and *e*) where clusters are relatively rare so we could be confident that they did not represent peripherally sectioned Golgi clusters. In fact only 3.5% of the vesicle labeling could be explained by labeling of peripherally sectioned clusters in the spindle (see Materials and Methods). Labeling was concentrated 16-fold (10 cell profiles, CV 82%) over vesicles, compared to the surrounding cytoplasm.

Metaphase Golgi Fragments

Clusters Vary in Number and Amount. The number of clusters in each cell was very variable during metaphase (Fig. 5). Overall the estimates varied from 10 to 308 clusters per cell (two cultures). The total volume of cluster in each cell also varied greatly during metaphase. For the three cultures examined, there was between 0.12 and 7.60 μm^3 of cluster per cell, with a mean of 2.74 μm^3 (CV 59%). Each culture examined showed the same marked variation in the cluster volume. One, for example, had a mean cluster volume

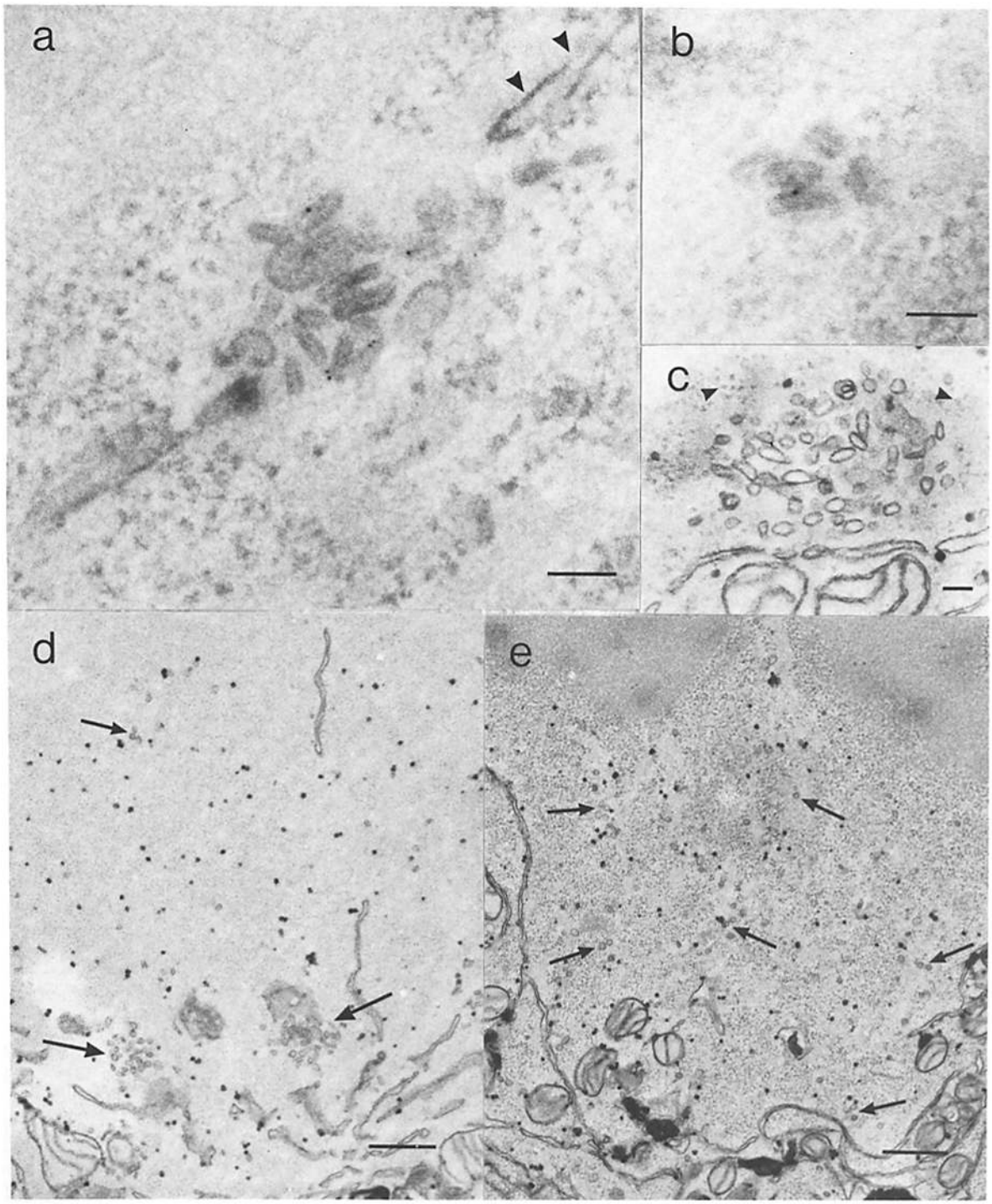

Figure 2. Metaphase clusters and vesicles. (*a* and *b*) Frozen sections; (*c*, *d*, and *e*) epoxy resin sections. The larger cluster in *a* is labeled for galactosyltransferase and is associated with a cisterna of the endoplasmic reticulum (*arrowheads*). Clusters with five vesicular profiles (*b*) were the smallest included in the quantitation of clusters. This cluster is labeled with a single gold particle. *c* shows a large cluster in a section used for stereological estimations. Membranes are well-visualized and ribosomes (*arrowheads*) are excluded from the cluster interior. *d* and *e* illustrate the vesicle density in spindle regions from cells with high and low volume fractions of Golgi cluster, respectively (*small arrows vesicles*, *large arrows clusters*). Bars: (*a–c*) 100 nm; (*d* and *e*) 500 nm.

of 2.23 μm^3 but the CV was 297% (10 cells). The marked variation of cluster number and volume in metaphase cells is illustrated in Fig. 6 *a* and is more obvious in the accompanying Log/Log plot (Fig. 6 *b*). Both figures show that the number and total volume of cluster are related. Cells with larger cluster numbers had larger cluster volumes (Fig. 6, *a* and *b*). This relationship held even when the cluster number and volume are expressed as densities (Fig. 6 *c*) showing it was not due to variation in cell size.

Estimates of cluster membrane surface in individual

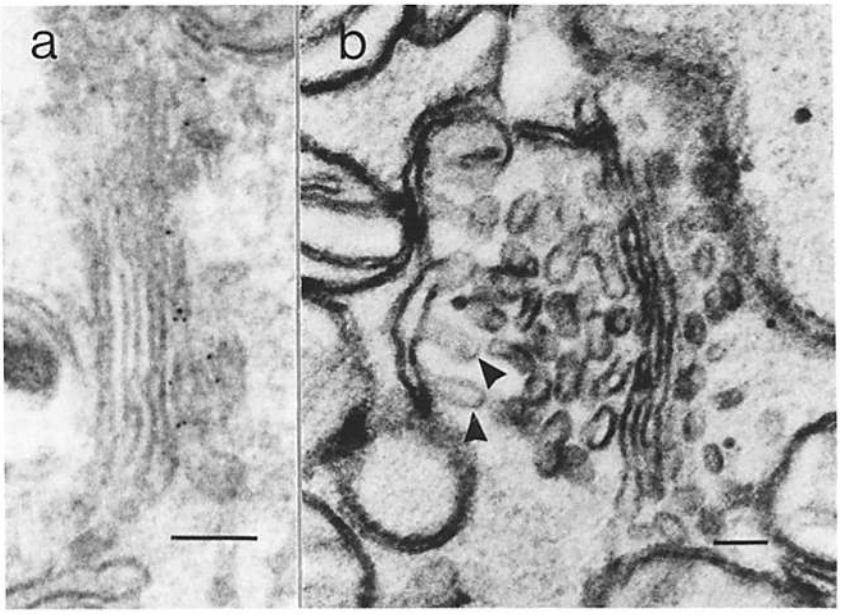

Figure 3. Dispersed reassembled Golgi stacks from telophase cells. (*a*) Frozen section; (*b*) epoxy resin section. In *a* the labeling for galactosyltransferase is found on one side of the cisternal stack and in *b* the cluster shows evidence of stack reassembly adjacent to buds of the endoplasmic reticulum (*arrowheads*). Bars, 100 nm.

metaphase cells varied in close accordance with the volume estimates. This is because the surface density of membrane in the clusters varied very little from cell to cell (see Materials and Methods). Therefore the total membrane surface also showed marked cell to cell variation, ranging from 4.9 to 239 μm^2 (see Fig. 9) with a mean of 86 μm^2 (three cultures, CV 44%). We should emphasize here that the cluster membrane surface areas are overestimates because the section thickness is close to the size of cluster vesicles. The actual values are likely to be less than this. In fact by applying a correction factor for the effect of section thickness to the mean gives a value of ~45 μm^2/cell. (This correction should be taken only as a guide because it is based on the assumption that all cluster vesicles have a spherical shape. This is true for most but not all cluster vesicles.)

The size distribution for Golgi clusters was obtained from serial section analysis of metaphase cells (Fig. 7). This was heavily skewed towards the smallest clusters (Fig. 7 *a*) so that those with a volume of 0.020 μm^3 or less were by far the most numerous (94%). Even so these small clusters contributed only 50% to the total cluster volume measured, the rest being contained within just a few larger clusters (Fig. 7 *b*).

The Number of Spindle Vesicles Is Inversely Related to the Amount of Cluster. A significant proportion of the galactosyltransferase labeling was found over spindle vesicles in frozen sections of metaphase cells (see above). An estimated 282 single gold particles were found over vesicles of the spindle amounting to 25% of the total (see Materials and Methods). This is clearly an underestimate of Golgi vesicle number because the efficiency of galactosyltransferase labeling in *trans*-Golgi vesicles is <100% and in addition some Golgi vesicles are likely to be derived from cisternae lacking galactosyltransferase. Because of these problems the number of Golgi vesicles was estimated using indirect, but independent, methods.

Table I. Galactosyltransferase Labeling in Golgi Clusters

Mitotic phase	Signal*	Background*	Signal/background ratio
Metaphase	20 (33%)	0.66 (33%)	31 (23%)
Telophase	27 (57%)	0.50 (35%)	53 (26%)

* Values are gold particles/μm^2.
Percentages in parenthesis are the coefficient of variation from three cultures.

An average of 8,000 vesicles were counted in the spindle of metaphase cells in unlabeled epoxy resin sections, of which a significant proportion could be derived from Golgi. We then found that the numerical density of these spindle vesicles was inversely related to the volume fraction of Golgi clusters in the cell (Fig. 8) so that those with the highest volume fraction (>0.0035) had a density of 19 vesicles/μm^3 (six cells, CV 44%) whereas those with the smallest volume fraction (<0.002) had 31 vesicles/μm^3 (12 cells, CV 27%). Spindle regions from cells belonging to each of these groups are shown in Fig. 2, *d* and *e*.

It is likely that this relationship reflected variation in the distribution of Golgi membrane between clusters and vesicles. It may therefore be used to derive the number of Golgi vesicles from the observed change in vesicle density for each unit change in cluster volume fraction. Each 0.001 change in cluster volume fraction represented 3.48 vesicles/μm^3 or 1,067 vesicles per cell for a spindle volume of 306 μm^3. Metaphase cells with the fewest vesicles (and most cluster) had a cluster volume fraction of ~0.006 compared to 0.0021 for the average metaphase cell. Conversion of clusters to vesicles over this range (total V_v 0.0039) would therefore yield ~4,000 Golgi vesicles per spindle and complete disassembly of the Golgi would yield at least 6,000 Golgi vesicles per spindle.

Estimates of vesicle number were also obtained using the labeling data assuming that the density of labeling over membrane is the same in the Golgi vesicles and clusters. This seems reasonable since the distinction between the clusters and vesicles is entirely artificial and they appear to be part of a continuous population of Golgi fragments (see the distri-

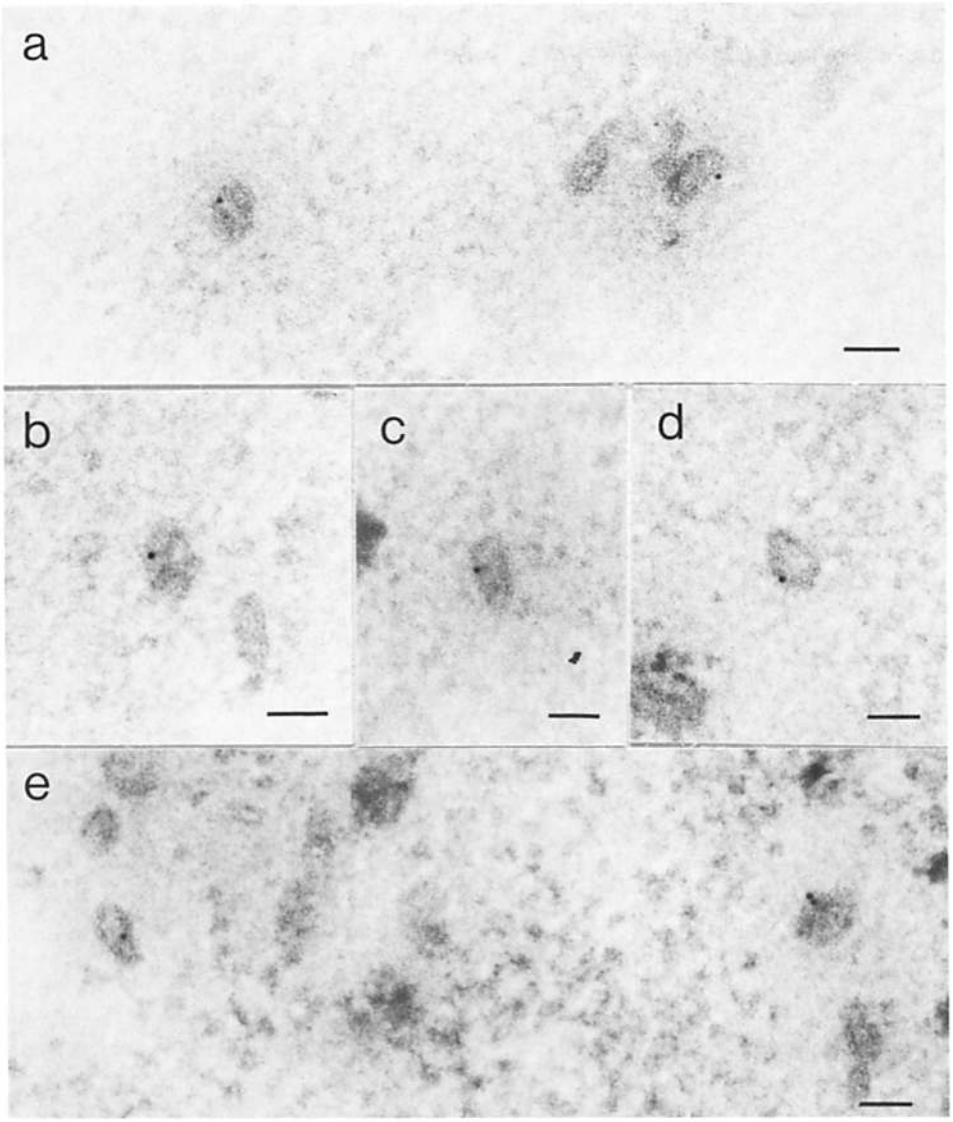

Figure 4. Free vesicles in frozen sections of metaphase cells. This is a gallery of vesicles from the mitotic spindles of metaphase cells labeled for galactosyltransferase. Gold particles are often found near the membrane of the vesicles. In *a* and *e* labeled vesicles are close enough to be included in the same micrograph. Bars, 50 nm.

bution of Fig. 7 *a*). Thus the clusters had a labeling density of 5.7 particles/μm^2 membrane (10.2 when corrected for sectioning effects on membrane density estimates). This gives an estimated surface area for spindle vesicles of 49.9 μm^2 (27.6 μm^2 corrected) and since the measured diameter of these vesicles is 57 nm (n = 16, CV 10.5%), the average metaphase cell would contain 4,900 (2,700 corrected) Golgi spindle vesicles.

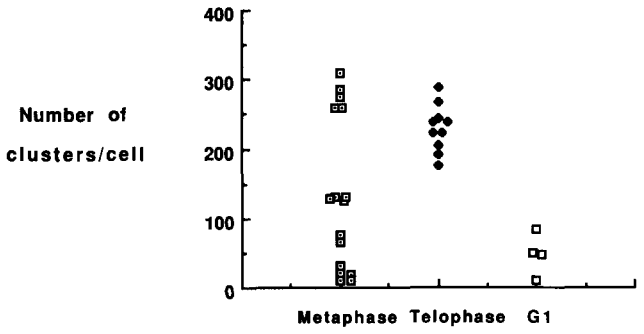

Figure 5. Number of Golgi clusters in metaphase, telophase, and G1 cells. Values are derived from two cultures. The number of clusters in each cell was counted using disectors placed systematic random through the cells. The number of clusters varies more in metaphase than in telophase and the number of clusters drops dramatically in early G1 cells.

Reassembly during Telophase

Telophase Clusters Acquire Membrane and Galactosyltransferase. The surface area of cluster membrane per cell is much higher in telophase than in metaphase cells (Fig. 9). Comparing the mean value of three cultures, telophase cells have over fourfold more cluster membrane. The actual ratio is probably larger than this because the membrane surface area of telophase clusters is not overestimated as much by the effect of section thickness (see Materials and Methods). The variation in surface area was much less than in metaphase so, for example, in a single, typical culture the mean cluster surface area per cell was 219 μm^2 with a CV of just 22% (six cells). For all cultures the mean estimated surface area was 356 μm^2/cell (n = 3, CV 31%) and after correction for the effect of section thickness was 230 μm^2/cell.

Galactosyltransferase labeling increased more than fivefold

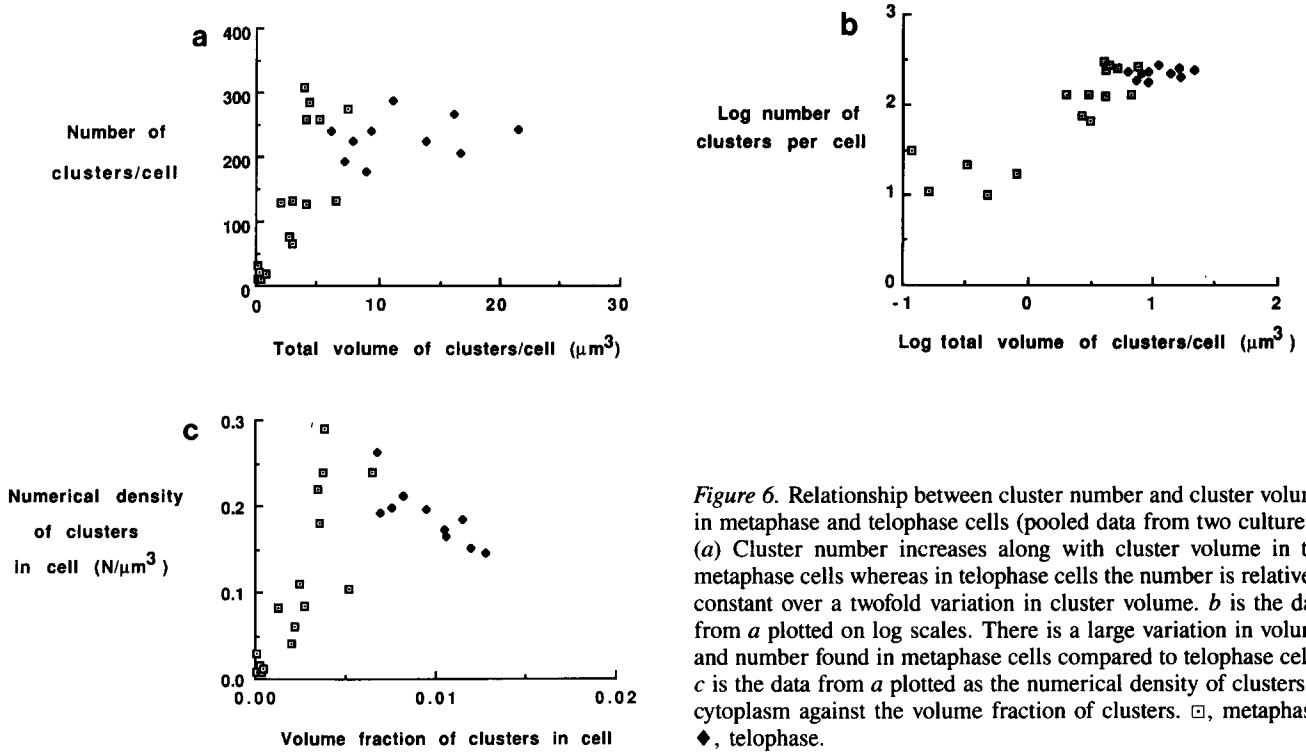

Figure 6. Relationship between cluster number and cluster volume in metaphase and telophase cells (pooled data from two cultures). (*a*) Cluster number increases along with cluster volume in the metaphase cells whereas in telophase cells the number is relatively constant over a twofold variation in cluster volume. *b* is the data from *a* plotted on log scales. There is a large variation in volume and number found in metaphase cells compared to telophase cells. *c* is the data from *a* plotted as the numerical density of clusters in cytoplasm against the volume fraction of clusters. ⊡, metaphase; ◆, telophase.

from 549 particles per cell in metaphase to 2,919 particles per cell in telophase.

The Spindle Vesicle Population Is Depleted during Telophase. The fraction of labeling over vesicular profiles dropped dramatically from 25% (three cultures, CV 38%) in metaphase to 1.4% (three cultures, CV 116%) in telophase corresponding to a drop in labeling from 183 to 41 gold particles per cell. This indicates that vesicular galactosyltransferase enters the clusters during reassembly although it cannot account for all of the increased immunolabeling seen in telophase clusters. This discrepancy may not only be due to the fact that peripheral sections of vesicles in the metaphase spindle are not visualized in frozen sections but also because the lumens of cisternae are more likely than small vesicles to be open on the labeled side of the section and therefore give easier access to antibodies. The increase in labeling is unlikely to be due to increased synthesis of galactosyltransferase because we were able to assay similar amounts of galactosyltransferase activity in mitotic and interphase cells (Lucocq et al., 1987).

There were ~8,000 vesicles in the spindle of each metaphase cell yet the total number of vesicles in each telophase cell was only ~2,000 showing clearly that the population of spindle vesicles is depleted during reassembly of the Golgi apparatus (Fig. 10). It is also interesting to note that those telophase cells with the lowest volume fraction of cluster in the cytoplasm had the largest number of free vesicles. This again indicates that vesicles are being incorporated into the reassembling Golgi apparatus.

Reassembly Occurs at a Limited Number of Sites. The

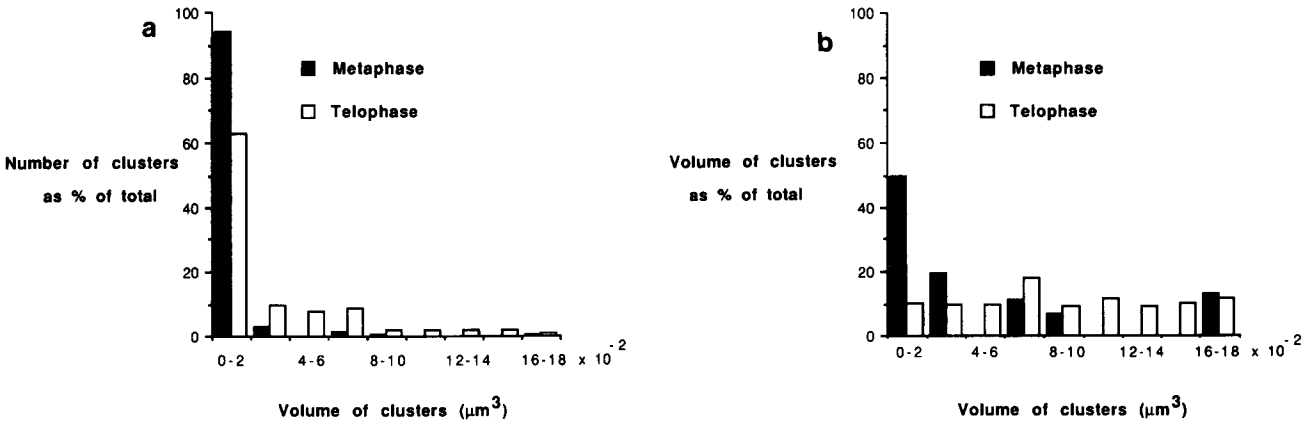

Figure 7. Relative number (*a*) and volume (*b*) of clusters in classes of cluster volume. (Data pooled from two cultures, three cells from each.) (*a*) The smallest clusters are most frequent in metaphase and telophase but telophase cells have a higher proportion of large clusters (see Results). (*b*) The small clusters of metaphase are the most numerous but comprise only about half of the total cluster volume, larger clusters holding the rest. In telophase, small clusters have only a small fraction of the volume because others have grown.

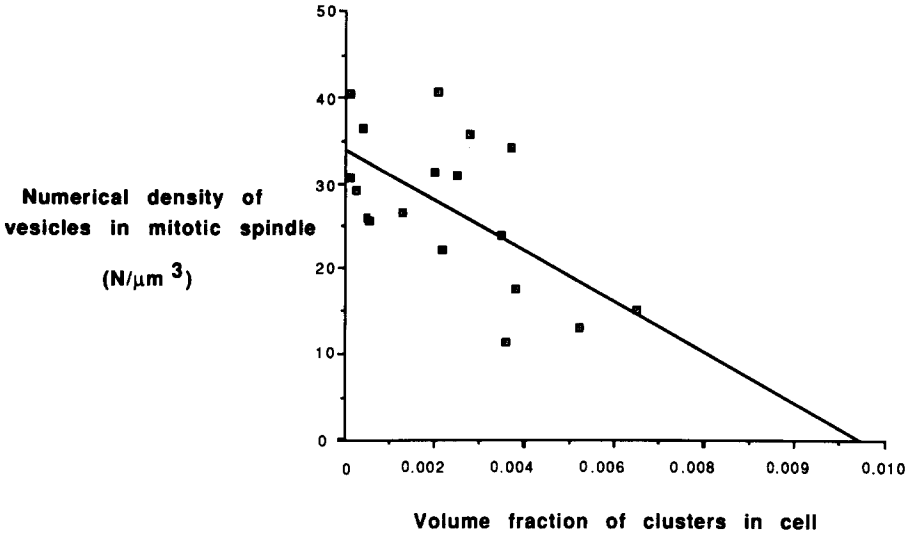

Figure 8. Relationship between the numerical density of vesicles in the metaphase spindle and the volume fraction of clusters in metaphase cells. Numerical density correlates significantly with the volume fraction ($r = -0.62$, $P < 0.01$).

total number of clusters per cell (Fig. 5) and the total cluster volume per cell (Fig. 6, *a* and *b*) are much more constant in telophase than in metaphase. The mean numbers per cell in two cultures were 222 (five cells, CV 9%) and 236 (five cells, CV 19%) giving an overall mean of 229. Many metaphase cells had fewer clusters than telophase cells, so new clusters must appear. However, the fourfold increase in membrane surface area (Fig. 9) did not result in four times the number of telophase clusters (Fig. 5). In fact, the number of telophase clusters per cell does not exceed the maximum found in metaphase cells. This indicates that the number of telophase clusters is limited and that they grow rather than many more of them being created de novo. Estimates on a population of individual clusters showed this to be the case (Fig. 11), the mean volume increasing from metaphase to telophase in two separate experiments, from 0.031 (eight cells, CV 60%) to 0.069 μm^3 (five cells, CV 32%) in one experiment, and from 0.022 (eight cells, CV 45%) to 0.04 μm^3 (five cells, CV 23%) in the other. Furthermore, a close correlation was found between the volume of individual clusters and the volume fraction in telophase cells (Fig. 12). Thus telophase cells with a larger cluster volume fraction make bigger clusters rather than more individuals. Interestingly the negative intercept on the ordinate indicates that the process of cluster growth is proceeding faster than the increase in volume fraction. This indicates that fusion of discrete clusters is occurring, a conclusion supported by the decrease in the numerical density of clusters with increasing volume density in Fig. 6 *c*.

The size distribution for Golgi clusters was obtained from serial section analysis of telophase cells (Fig. 7). Whereas 63% of the number was found in the smallest size class (0–0.020 μm^3) the rest were distributed in all of the larger size classes up to 0.18 μm^3 (Fig. 7 *a*). In contrast only 10%

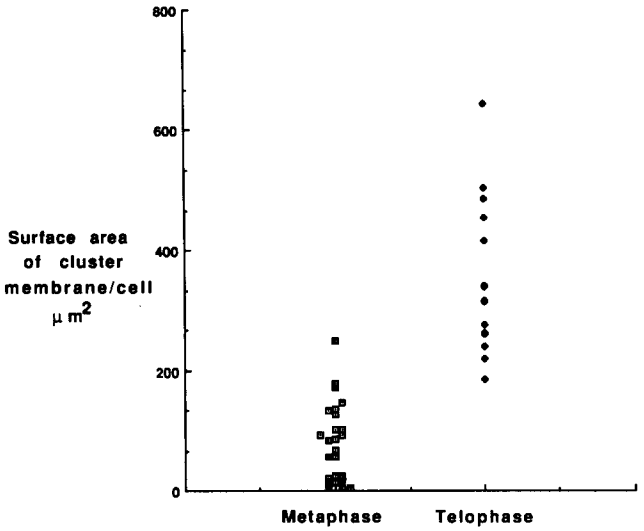

Figure 9. Membrane surface area in the clusters of metaphase and telophase cells. Values are pooled from three cultures. There is an increase of membrane surface area per cell from metaphase to telophase. The values are uncorrected for the effect of section thickness (see Results).

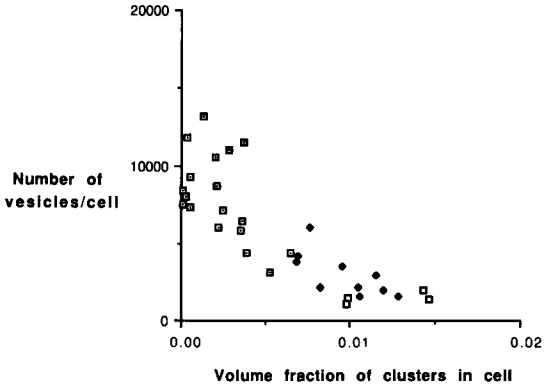

Figure 10. The number of vesicles per cell in metaphase spindles and telophase and G1 cells is plotted against the volume fraction of cluster in the cell. Metaphase cells with the greater concentration of cluster have the least spindle vesicles and vice versa. In telophase and G1 cells the number of vesicles per cell is greatly reduced but those telophase cells with the lowest volume fraction of clusters have most vesicles. ⊡, metaphase (spindle vesicle); ♦, telophase (all vesicles; □, G1.

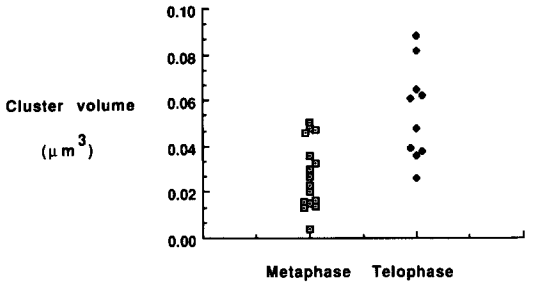

Figure 11. Mean volumes of clusters in metaphase and telophase cells. (Data pooled from two cultures.) The volume of the clusters increases from metaphase to telophase.

of the volume was found in the smallest size class which was similar to the percentage found in all other size classes (Fig. 7 *b*). These results were markedly different from those obtained using metaphase cells and suggest that growth of the clusters is nonuniform.

Cisternae Appear within Dispersed Clusters. Only a minority of metaphase clusters contained cisternae (4.3%, n = 209) whereas more than half of the telophase clusters (58%, n = 130) had them. The number of clusters containing cisternae was estimated to be ~135 per cell.

Quantitation of galactosyltransferase labeling showed that 83% was in Golgi clusters containing cisternae whereas 93% of all clusters containing cisternae were labeled. Further analysis revealed that clusters containing cisternae had 95% of the cluster volume and therefore contained most of the cluster membrane. Telophase clusters containing cisternae must therefore be the major sites of Golgi reassembly.

The Role of Putative Transitional Element Regions of the Endoplasmic Reticulum. The transitional element region of the endoplasmic reticulum is closely apposed to the Golgi stack in interphase cells. It is characterized by bud-like profiles on the rough endoplasmic reticulum (Palade, 1975). In serial sections of interphase HeLa cells we found that the rough endoplasmic reticulum buds were located primarily in the Golgi region of the cell. In a series of 20 serial sections from the bottom of a monolayer the buds were present in groups on the endoplasmic reticulum and 78% of these groups (n = 100 from four cells) were present adjacent to the Golgi stacks. (Incidentally because the Golgi-associated groups contained most buds this number is still an underestimate for the proportion of buds in the Golgi region.) We therefore consider these buds to be characteristic of the Golgi region of HeLa cells and they probably correspond to the transitional element buds described by other authors. In metaphase cells only 21% (n = 209) of the clusters contained transitional element buds whereas 58% (n = 130) of the telophase clusters had them. This increased to 82% (n = 78) when clusters with cisternae alone were considered. This shows that buds are a characteristic feature of the dispersed Golgi stacks as they reassemble in telophase.

Fusion of Clusters To Form the Juxtanuclear Golgi Complex. Clusters congregated next to the nucleus in early G1 cells. These cells had a reduced number of clusters counted with the disector method (Fig. 5) indicating that they had fused.

Discussion

Golgi Fragments in Metaphase Cells

Using immunoelectron microscopy we have identified two types of Golgi fragment produced by disassembly of the interphase Golgi apparatus during mitosis in HeLa cells. These are tubulovesicular Golgi clusters and a new type of fragment, free vesicles. Golgi clusters have already been described in HeLa cells embedded in Lowicryl K4M (Lucocq et al., 1987) but we have now identified much smaller clusters because cluster vesicles are well-visualized in frozen sections. Clusters with as few as five component vesicle profiles could be identified while even smaller clusters and many single vesicle profiles were also labeled for galactosyltransferase and were assigned to a "free vesicle" population. The boundary between the smallest clusters and the free vesicle population is of course entirely artificial. In fact clusters and free vesicles probably form a continuous population, as is suggested by the progressive increase in cluster number with decreasing size (Fig. 7 *a*).

The total Golgi cluster volume and membrane surface varied considerably from cell to cell and many of the metaphase cells contained only small amounts of Golgi cluster and large numbers of vesicles. An average metaphase cell was found to contain 34.1 μm^2 of membrane surface area[2] as vesicles and 45 μm^2 as clusters. In a previous publication we discussed the possibility that Golgi clusters are involved in partitioning Golgi membrane between daughter cells during mitosis (Lucocq and Warren, 1987). Golgi vesicles may also perform this function. They contain enough Golgi membrane (in most metaphase cells) for them to have an important influence on the final distribution of Golgi apparatus and since there are thousands of them in an average metaphase cell, random partitioning would ensure an almost equal distribution between daughter cells (Lucocq and Warren, 1987). Whichever type of Golgi fragment has a partitioning function only furthur work will establish in which mitotic stages and by which mechanism it is committed to enter daughter cells.

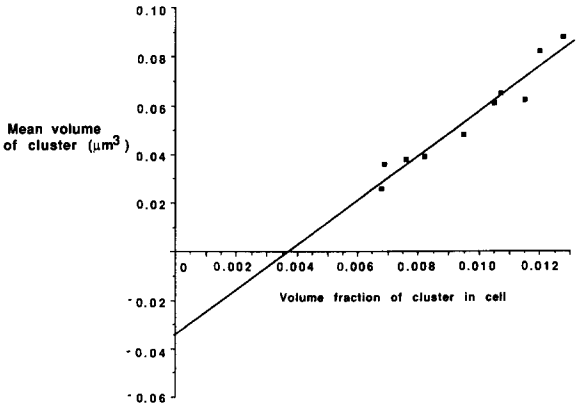

Figure 12. Cluster volume correlates with the volume fraction of clusters in telophase cytoplasm (r = 0.97, $P < 0.001$). Interestingly the ordinate intercept is less than zero indicating that some cluster fusion is occurring.

2. Mean obtained using two independent estimates of Golgi vesicle number (see Results).

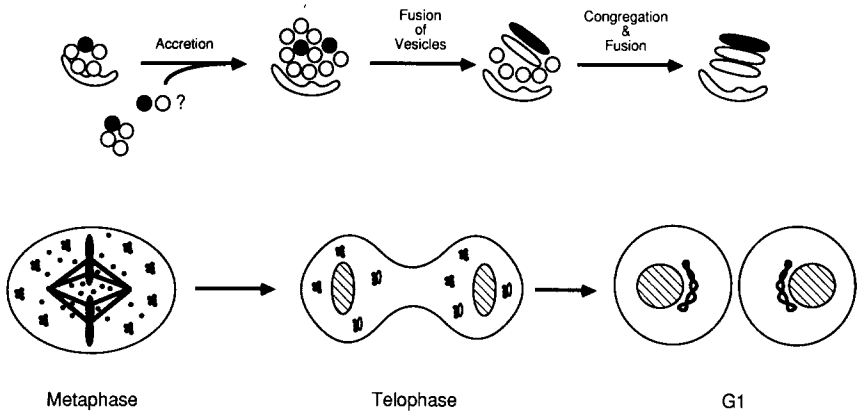

Figure 13. A model of Golgi division. The reassembly pathway involves accretion of vesicles and their fusion to form cisternal stacks at a limited number of sites on the endoplasmic reticulum. The dispersed stacks subsequently congregate and fuse in the juxtanuclear region to form the interconnected Golgi stack of interphase cells. The disassembly steps that produce clusters and vesicles have yet to be characterized.

Reassembly Pathway

The data presented in this paper shows that reassembly of the Golgi apparatus in telophase involves at least two steps (see Fig. 13). The first step involves formation of the many dispersed cisternal clusters that are rebuilt close to the endoplasmic reticulum. They grow individually, probably by accretion of free vesicles and also some clusters. The total surface area of membrane contributed by these fragments is ~85 μm^2/cell which is substantially less than our estimate of 230 μm^2/cell for the total surface of membrane in the telophase cisternal clusters. The extra membrane could be contained in the 4,000 or more vesicles of the spindle that we cannot at present assign to the Golgi vesicle population, perhaps due to limitations in our techniques. Alternatively the endoplasmic reticulum could be the source of membrane because transport from the endoplasmic reticulum to the Golgi apparatus is arrested in mitotic cells (Featherstone et al., 1985) but recommences in telophase.

The rebuilding of Golgi apparatus cisternal stacks in telophase must be a very complex process. Not only must vesicles destined to reassemble a particular Golgi subcompartment recognize each other but there must also be a "template" for recreating the proper order of cisternae in the stack. Each "template" might only require a single representative (vesicle) from each of the known cisternal compartments (*cis*, *medial*, *trans*). In other words, a metaphase cluster with three vesicles might be sufficient to retain the information necessary to reconstitute the stack. We would therefore expect to find several hundred clusters of three or more in metaphase cells. Unfortunately, identification of such small clusters is problematic because (*a*) we do not have markers for *cis* and *medial* cisternae, (*b*) sectioning does not visualize all three vesicle clusters, and (*c*) only a small fraction of such small clusters will be labeled because immunoelectron microscopy is not 100% efficient. In this study we could only reliably identify clusters with a minimum of five vesicles in their profiles and some metaphase cells had much less than a hundred of these. Further work will therefore be needed to identify possible templates for reassembly.

But why reassemble multiple Golgi stacks? One possibility is that functioning, reassembled stacks are required in telophase before partitioning of the Golgi apparatus can occur. In this case metaphase clusters and vesicles would not be involved in partitioning. Instead the 100 or more dispersed cisternal clusters would ensure the Golgi is distributed equally between each daughter cell. Another possibility is that the dispersed telophase cisternal clusters represent subunit structures of the Golgi apparatus. Perhaps these can be best observed in telophase because at this stage the cells lack the mechanism that later translocates them to the juxtanuclear region where they fuse to form the typical single copy Golgi apparatus of interphase cells.

The second step in Golgi reassembly is the congregation of stacks in the juxtanuclear region of the cell and their fusion to form the interphase Golgi stack. At present the driving force for translocation is not known but it is possible that movement along microtubules is involved since a microtubule binding protein has been found associated with Golgi apparatus membrane (Allan and Kreis, 1986).

Disassembly Pathway

In contrast to Golgi reassembly we understand little of the disassembly pathway that generates the two types of Golgi fragment we have described. Although we have not studied the earliest steps of disassembly our data does give us insights into the relationship between clusters and vesicles. The simplest model is one in which vesicles are reversibly shed from the clusters as is suggested by the inverse relationship between the density of Golgi vesicles and the cluster volume fraction. However, it may be more realistic to explain the disassembly in terms of the fragment size distributions because the populations of clusters and vesicles appear to be continuous (Fig. 7). Disassembly could be seen simply as a shift in the distribution of fragment size and number. As disassembly proceeds it produces smaller and smaller fragments with larger and larger numbers, perhaps because smaller clusters are more stable than larger ones. Interestingly, in a few metaphase cells, the distribution has moved further towards smaller structures than in others. This could be due to different rates of disassembly or due to the fact that we sampled cells at different time points during metaphase. Whatever the explanation there must be factors that drive the distribution toward smaller structures and these must be active only during specific periods of mitosis. Conceivably, they could act at the level of the matrix in which both interphase (Mollenhauer and Morre, 1978) and mitotic Golgi structures (Lucocq et al., 1987) are embedded. The nature of such factors and the exact pathway of Golgi disassembly

will only be discovered once the morphological and biochemical studies of the early mitotic stages have been carried out.

In summary we have started to construct a morphological map of Golgi division. Clearly disassembly and reassembly of the Golgi involve specific proteins that function at each of the steps we have described. We hope to use this map to reconstitute parts of the division process in vitro so that the proteins involved can be identified and their functions characterized.

We thank Dr. T. Mayhew for his interest, advice, and helpful discussions concerning the stereology and Dr. J. Paulson for the gift of the anti-rat sialytransferase antiserum. The technical assistance of Mrs. C. Lyons and Mr. K. Leask are gratefully acknowledged and we thank Drs. J. Pryde and P. Woodman for critical reading of the manuscript. Lastly we would like to thank Prof. H. J. G. Gundersen whose review greatly improved the paper.

This work was supported by grant number SP 1757 from the Cancer Research Campaign.

Received for publication 4 November 1988 and in revised form 18 April 1989.

References

Allan, V. J., and T. E. Kreis. 1986. A microtubule-binding protein associated with membranes of the Golgi apparatus. *J. Cell Biol.* 103:2229–2239.

Burke, B., G. Griffiths, H. Reggio, D. Louvard, and G. Warren. 1982. A monoclonal antibody against a 135K Golgi membrane protein. *EMBO (Eur. Mol. Biol. Organ.) J.* 1:1621–1628.

Cochran, W. G. 1977. Sampling Techniques. John Wiley & Sons Ltd., London.

Featherstone, C., G. Griffiths, and G. Warren. 1985. Newly synthesized G protein of vesicular stomatitis virus is not transported to the Golgi complex in mitotic cells. *J. Cell Biol.* 101:2036–2046.

Galey, F. R., and S. E. G. Nilsson. 1966. A new method for transferring sections from the liquid surface of the trough, through staining solutions to the supporting film of a grid. *J. Ultrastruc. Res.* 14:405–410.

Gundersen, H. J. G. 1977. Notes on the estimation of the numerical density of arbitrary profiles: the edge effect. *J. Microsc. (Oxf.).* 111:219–223.

Gundersen, H. J. G. 1986. Stereology of arbitrary particles. *J. Microsc. (Oxf.).* 143:3–45.

Hiller, G., and K. Weber. 1982. Golgi detection in mitotic and interphase cells by antibodies to secreted galactosyltransferase. *Exp. Cell Res.* 142:85–94.

Keller, G. A., K. T. Tokuyasu, A. H. Dutton, and S. J. Singer. 1984. An improvement procedure for immunoelectron microscopy: ultrathin plastic embedding of immunolabelled ultrathin frozen sections. *Proc. Natl. Acad. Sci. USA.* 81:5744–5747.

Lucocq, J. M., and G. Warren. 1987. Fragmentation and partitioning of the Golgi apparatus in HeLa cells. *EMBO (Eur. Mol. Biol. Organ.) J.* 6:3239–3246.

Lucocq, J. M., J. Pryde, E. Berger, and G. Warren. 1987. A mitotic form of the Golgi apparatus in HeLa cells. *J. Cell Biol.* 104:865–874.

Mollenhauer, H. H., and D. J. Morre. 1978. Structural compartmentation of the cytosol: zones of adhesion, cytoskeletal and intercisternal elements. *Subcell. Biochem.* 5:327–359.

Novikoff, P. M., A. B. Novikoff, N. Quintana, and J.-J. Hauw. 1971. Golgi apparatus, GERL, and lysosomes of neurons in rat dorsal root ganglia, studied by thick section and thin section cytochemistry. *J. Cell Biol.* 50:859–886.

Rambourg, A., Y. Clermont, and A. Marraud. 1974. Three-dimensional structure of the osmium-impregnated Golgi apparatus as seen in the high voltage electron microscope. *Am. J. Anat.* 140:27–46.

Rambourg, A., Y. Clermont, and L. Hermo. 1979. Three-dimensional architecture of the Golgi apparatus in Sertoli cells of the rat. *Am. J. Anat.* 154:455–476.

Rambourg, A., Y. Clermont, and L. Hermo. 1981. Three-dimensional structure of the Golgi apparatus. *Methods Cell Biol.* 23:155–166.

Roth, J., and E. Berger. 1982. Immunocytochemical localization of galactosyltransferase in HeLa cells: codistribution with thiamine pyrophosphatase in *trans*-Golgi cisternae. *J. Cell Biol.* 83:223–229.

Small, J. V. 1968. Measurement of section thickness. *In* Proceedings of the 4th European Congress on Electron Microscopy. D. S. Bocciarelli, editor. Tipografia Poliglotta, Rome, Italy. 609–625.

Sterio, D. C. 1984. The unbiased estimation of number and sizes of arbitrary particles using the disector. *J. Microsc.* 134:127–136.

Weibel, E. R., and D. Paumgartner. 1978. Integrated stereological and biochemical studies on hepatocyte membranes. II. Correction of section thickness effect on volume and surface density estimates. *J. Cell Biol.* 77:584–597.

Zeligs, J. D., and S. H. Wollman. 1979. Mitosis in rat thyroid epithelial cells in vivo. I. Ultrastructural changes in cytoplasmic organelles during the mitotic cycle. *J. Ultrastruc. Res.* 66:53–77.